

## Low-Energy Linear Structures in Dense Oxygen: Implications for the $\epsilon$ Phase

J. B. Neaton<sup>1</sup> and N. W. Ashcroft<sup>2,3</sup>

<sup>1</sup>*Department of Physics and Astronomy, Rutgers University, Piscataway, New Jersey 08854-8019*

<sup>2</sup>*Laboratory of Atomic and Solid State Physics and Cornell Center for Materials Research, Cornell University, Ithaca, New York 14853-2501*

<sup>3</sup>*Cavendish Laboratory, University of Cambridge, Madingley Road, Cambridge, CB3-0HE, United Kingdom*

(Received 25 January 2002; published 3 May 2002)

Using density functional theory implemented within the generalized gradient approximation, a new nonmagnetic insulating ground state of solid oxygen is proposed and found to be energetically favored at pressures corresponding to the  $\epsilon$  phase. The newly predicted static ground state is composed of linear herringbone-type chains of O<sub>2</sub> molecules and has *Cmcm* symmetry (with an alternative monoclinic cell). Importantly, this phase supports IR-active zone-center phonons, and their computed frequencies are found to be in broad agreement with recent infrared absorption experiments.

DOI: 10.1103/PhysRevLett.88.205503

PACS numbers: 62.50.+p, 61.50.Ah, 78.30.Am

At low temperatures and ordinary pressures oxygen condenses into the only antiferromagnetic insulating phase known among the elemental solids. In its ground state, the well-known monoclinic  $\alpha$  phase [1], the molecular spins are arranged in nearly close-packed planes (or layers) perpendicular to the molecular axes; the axes of molecules in successive planes are collinear [1–3] (and apparently so in *all* measured phases). As the temperature is increased, oxygen eventually undergoes a transition to its familiar room-temperature gaseous phase; as *pressure* is increased, however, its attributes depart radically from those of an ensemble of weakly interacting molecules. In fact, at pressures above 96 GPa (nearly threefold compression), both diamond-anvil [4,5] and shock [6] experiments have reported an insulator-metal (IM) transition and, at temperatures below 0.6 K, the metallic state (the  $\zeta$  phase) even exhibits superconductivity [7]. While some of the broader aspects of the electronic behavior are understood throughout this density range, the crystal structure and magnetic properties of the so-called  $\epsilon$  phase, persisting as it does over the wide, intermediate pressure range of 10–96 GPa, remain unknown.

Over two decades ago, a dramatic color change was observed (from light-blue transparent to darkening red) in experiments above 10 GPa at room temperature [8]. Detailed optical measurements [2] thereafter at room temperature revealed an abrupt onset of infrared (IR) absorption in the fundamental molecular vibron, also at approximately 10 GPa. Recent low-frequency optical studies have uncovered another strong IR peak, ranging in frequency between 300–500 cm<sup>-1</sup> from 10 to 70 GPa, but at very much lower frequencies than that of the vibron [9–11]. The formation of *pairs* of O<sub>2</sub> molecules with *D*<sub>2h</sub> (rectangular) symmetry—an O<sub>4</sub> unit—has been suggested to explain these new low-frequency modes [9,11]. Interestingly enough, the sudden increase in the intensity of infrared activity in two quite different frequency bands parallels the case of dense hydrogen, where a spontaneous polarization of the charge density

along the molecular bonds has been suggested to account for the stability of low-symmetry structures above 150 GPa [12].

Although there exist several promising structures [9,10,13–17], to date x-ray diffraction studies have been unable to completely reveal the exact positions of the molecules in the  $\epsilon$  phase. Likewise a previous first-principles study recorded a premature magnetic collapse and concomitant metallization into the  $\zeta$  phase near 12 GPa [18], bypassing the  $\epsilon$  phase. In this Letter we summarize the results of first-principles calculations that predict a new low-enthalpy molecular arrangement in the pressure range of the  $\epsilon$  phase. Beginning with a symmetric low-density structure, we observe that it is *unstable* to the formation of extended herringbone-type chains of O<sub>2</sub> molecules (instead of O<sub>4</sub> units), strikingly similar to that suggested by Agnew *et al.* [15]. Nonmagnetic and insulating, this newly predicted phase is also consistent with recent infrared measurements [9–11].

We examine here the stability of the common symmetric phases of oxygen over the molar volume range 6.7–13 cm<sup>3</sup>/mole, the lower value corresponding to pressures exceeding 100 GPa. Density functional theory is used within the local spin-density approximation (LSDA) [19] and with gradient corrections [20]. We utilize the projector augmented-wave (PAW) method [21] as implemented within the Vienna *ab initio* simulations package [22]. Our oxygen PAW potential relegates the 1s electrons to a frozen core but otherwise treats all other electrons explicitly as valence; a 60 Ry plane wave cutoff is used for all calculations. These methods provide a particularly accurate picture of the free molecule for which we correctly obtain the magnetic (*S* = 1) ground state; our calculated bond length of 1.236 Å, binding energy of near 6.0 eV, and molecular vibron frequency of 1550 cm<sup>-1</sup> are all slightly larger than experiment (1.207 Å) but quite consistent with the known tendency of gradient corrections to overestimate the bond length and binding energy of *p*-bonded diatomic molecules [23].

A primary physical issue centers on the notably high linear dipole polarizability of the oxygen molecule. The *along-axis* tensor component is  $15.9a_0^3$  and the *off-axis* components are  $8.2a_0^3$  [24], where  $a_0$  is the Bohr radius. These exceed the corresponding quantities in hydrogen by more than a factor of 2, and the Hertzfeld criterion (for the onset of a polarization divergence) would require a compression of only about 1.8. There is a large anisotropic fluctuating-dipole (or van der Waals) attraction [25], and an accurate, effective, and fully nonlocal representation of these correlated fluctuations within density functional theory has proven to be a challenge [26,27]. Thus the local density approximation is not expected to be satisfactory until significant intermolecular density has accumulated, and accordingly we focus our study on volumes less than  $13 \text{ cm}^3/\text{mole}$  (8 GPa), above which we obtain adequate agreement ( $\pm 5 \text{ GPa}$ ) with the equation of state at 300 K [4].

At room temperature and under a moderate compression of 8 GPa, the antiferromagnetic  $\delta$  phase (space group *Fmmm*) of solid oxygen has been particularly well characterized [2,3,8]. However recent x-ray data suggest a direct  $\alpha$ -to- $\epsilon$  transition at low temperatures [16]. Further, IR [10] and Raman [28] spectra between 2–8 GPa and below 20 K appear to be inconsistent with *Fmmm* symmetry. Thus in order to examine the possibility of lower symmetry ground states that *do* possess IR activity at the observed frequencies, we released the symmetry constraints of a four-molecule *Fmmm* orthorhombic cell and *completely relaxed the internal coordinates and lattice parameters*, all with dense  $\mathbf{k}$ -point sampling. This immediately resulted in a significant rearrangement of the crystal and in a new, stable orthorhombic structure, possessing a two-molecule primitive cell and *Cmcm* space-group symmetry. A plot of the enthalpies as a function of pressure for all structures considered appears in Fig. 1. For comparison, we also evaluate the enthalpy of the *metallic C2mm* phase, a candidate  $\zeta$  phase proposed by Serra *et al.* [18]. Interestingly, we find the *Cmcm* structure to be unstable to *C2mm* at a calculated pressure of 47 GPa, resulting in an IM transition at a lower pressure than experimentally observed (96 GPa [4]). Since the IM transition is associated with band gap closure, this discrepancy may result from the usual underestimate of the electronic band gap by the gradient-corrected LSDA.

Atomic arrangements for the three phases considered here appear in Fig. 2. In the *Cmcm* structure the oxygen molecules order into symmetric herringbone-type chains along [010] (the  $b$  axis) and *perpendicular* to the molecular bonds. They form through the shearing of adjacent (010) planes of the *Fmmm* structure, reducing the coordination of the molecules from four to two. An  $\epsilon$  phase having monoclinic symmetry has been suggested [3,4,16], and in this context we note that a monoclinic primitive lattice vector  $\mathbf{c}'$  can be chosen for *Cmcm* (where  $|\mathbf{c}'| = \frac{1}{2}\sqrt{a^2 + c^2}$ ). [A similar relationship exists between the  $\alpha$  (*C2/m*) and  $\delta$  (*Fmmm*) phases [16].] Nevertheless we find that distor-

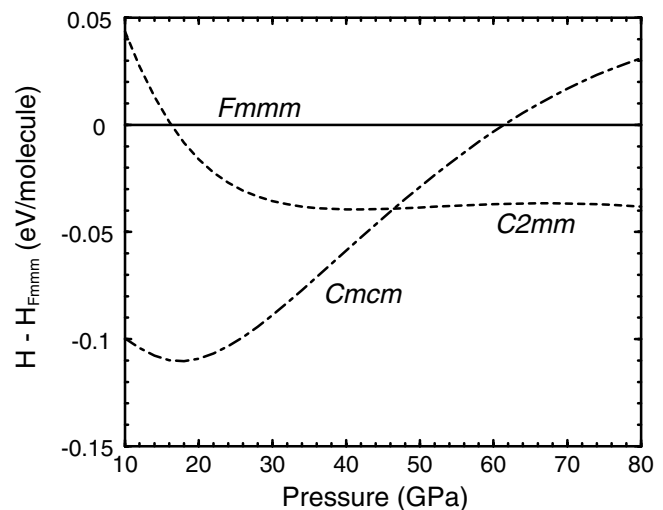


FIG. 1. Enthalpy ( $H = E + pV$ ) vs pressure  $p$  for selected structures of dense oxygen with respect to the *Fmmm* phase at  $T = 0 \text{ K}$ . In general agreement with a previous study [18], we observe that the *Fmmm* phase is unstable to *C2mm* above 17 GPa. Convergence with respect to  $\mathbf{k}$  points is achieved at 1 meV/molecule using  $10 \times 10 \times 12$  Monkhorst-Pack  $\mathbf{k}$  meshes for two-molecule primitive cells; more  $\mathbf{k}$  points are used for the metallic phase. Hellmann-Feynman forces are fully relaxed toward equilibrium positions until less than  $10^{-2} \text{ eV/\AA}$ .  $E(V)$  is well fit to  $\sum_{n=-2}^2 a_n V^{-n/3}$ .

tions of its orthorhombic lattice vectors  $\mathbf{a}$  and  $\mathbf{c}$  (resulting in  $P2_1/c$  symmetry) do not lower the total energy [29]. The *Fmmm* phase is related through continuous distortion to the nearly close-packed *C2mm* phase by a displacement of (001) planes in the [100] direction [30]. Interestingly, the dimer length is found to decrease by about 1% with increasing pressure in this new phase, from 1.224 Å at 8 GPa to 1.209 Å at 54 GPa. The distance between neighboring molecules along the chain is reduced from 2.081 Å

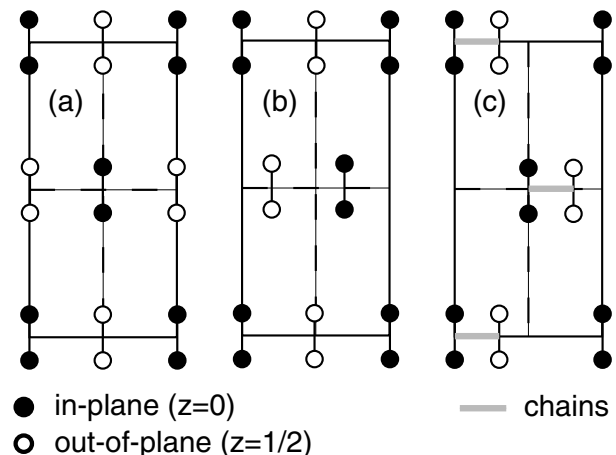


FIG. 2. Schematics of (010)  $ac$  planes of (a) *Fmmm*, (b) *C2mm*, and (c) newly predicted *Cmcm* phases. The molecules in white (oriented along [001]) are shifted by half a lattice vector out of the plane. The orthorhombic *Cmcm* phase [having Wyckoff positions 8(g)] results from an intraplanar distortion in which the center molecule moves off site. Chains run perpendicular to the plane and are indicated by bold gray lines. Differences in, e.g.,  $a$  or  $c/a$  are ignored in these illustrations.

to 1.986 Å over this range, a modest overbinding with respect to experiment, where these distances are thought to be in the range 2.2–2.5 Å [9]. Similarly, the  $a$ ,  $b$ , and  $c$  lattice parameters decline from 3.805 to 3.333 Å, 2.990 to 2.718 Å, and 7.034 to 6.216 Å, respectively, as pressure is increased from 8 to 54 GPa. Notably,  $c$  diminishes slightly faster than either  $a$  or  $b$  with increasing pressure; experimentally, the  $b$  axis is observed to decrease most rapidly [10]. Since the  $c$ -axis spacing is much larger than either  $a$  or  $b$ , remnant van der Waals interactions (see above) may still be particularly important between adjacent (001) planes, and therefore it is here that our treatment of exchange and correlation is likely to be most inadequate.

Solid oxygen is robustly insulating in the  $Cmcm$  structure, and the calculated band gap (a considerable underestimate of the true band gap) decreases from 0.95 eV (direct gap) near 8 GPa to about 0.55 eV (indirect gap) at ~55 GPa. The optical threshold of the  $\epsilon$  phase has been measured to be about 3 eV (blue-violet) near 10 GPa, declining to ~2.0 eV (red) near 55 GPa [5], for light polarized perpendicular to the molecular axis. These are larger than our computed direct gaps at these pressures (for the smallest, by a factor of 3) but, as stated above, this is to be expected given our use of the LSDA; corrections through approximate inclusion of many-electron effects via, for example, the  $GW$  approximation [31] would be of considerable interest for accurately reproducing this gap and likewise describing the onset of metallization.

The charge density is plotted in Fig. 3 in the  $ab$  plane (perpendicular to [001]), and is seen to develop an asymmetry occurring perpendicular to the molecular bond but centered on each molecule, providing insight into the stability of this phase. The asymmetry may be viewed as a weakly antiferroelectric state, whose physical origin may

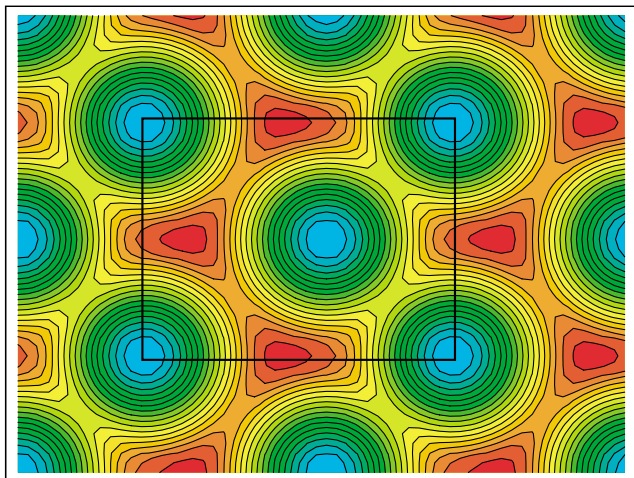


FIG. 3 (color). Charge density slice of  $Cmcm$  at a calculated pressure of 20 GPa ( $10.26 \text{ cm}^3/\text{mole}$ ) plotted in a (001) (or  $ab$ ) plane passing through the molecular centers (the unit cell is outlined in black). A natural logarithmic scale is used; the highest contours (blue) are 54 times larger than the lowest (red). Since the chains are equally spaced in the cell, the development of an alternating polarization *perpendicular* to the molecule is evident by inspection.

in turn be understood through consideration of a mean-field argument for a dynamic lattice as given for hydrogen [12]. Thus self-consistent Lorenz fields compensate energetic costs associated with the low-symmetry  $Cmcm$  structure in the intermediate pressure range below 50 GPa. Increasing intermolecular overlap at higher densities lowers kinetic and exchange energies, and the metallic  $C2mm$  phase is thus eventually favored. Examination of the spin density indicates that oxygen is *nonmagnetic* within this phase, consistent with inferences from other studies [9,32]; total energies and forces obtained from spin- and non-spin-polarized calculations are essentially identical.

Since there are two molecules in each primitive  $Cmcm$  cell, we expect nine optical phonons (plus three purely translational modes). At the zone center, there are eight irreducible representations, as permitted by the  $D_{2h}$  point group: four allow Raman activity ( $A_g$ ,  $B_{1g}$ ,  $B_{2g}$ , and  $B_{3g}$ ), three are IR active ( $B_{1u}$ ,  $B_{2u}$ , and  $B_{3u}$ ), and a single remaining  $A_u$  mode is silent. (The  $B_{1u}$  mode is purely translational.) Gorelli *et al.* [9,11] proposed a structure made up of two molecules (actually  $O_4$  units) having  $D_{2h}$  symmetry. In agreement with Ref. [11], our predicted ground state possesses  $D_{2h}$  point symmetry, but also includes additional lattice translations associated with the herringbone-type chain structure. Corresponding force constants are obtained through analysis [33] of a series of frozen-phonon calculations; phonon frequencies are then computed by diagonalization of block-diagonal dynamical matrices.

The pressure dependence of zone-center optical frequencies computed between 8 and 86 GPa appears in Fig. 4, and we obtain remarkably good agreement with the existing spectroscopic data, quite apart from the fact that  $C2mm$  is favored above 47 GPa in our calculations. Consistent with observations [11], we predict two IR-active modes over this range. The  $B_{3u}$  mode is an antiphase

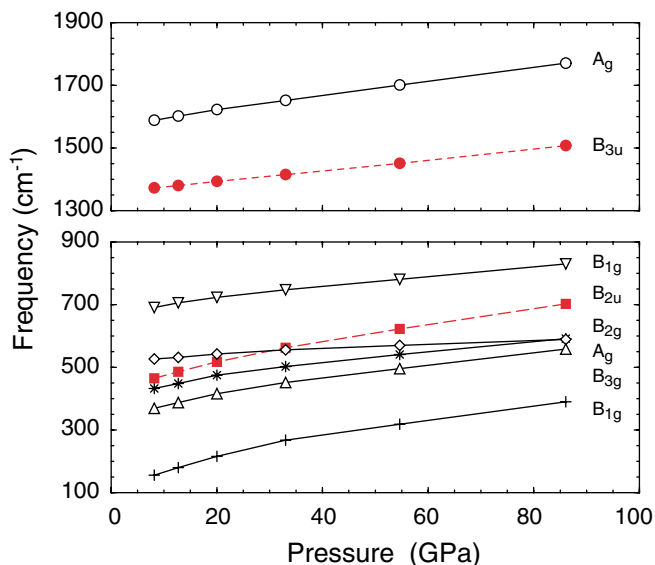


FIG. 4 (color). Calculated zone-center phonons of  $Cmcm$  as a function of pressure. Modes having  $B_{2u}$  and  $B_{3u}$  symmetry are IR active (red dashed lines); the remaining are Raman active (black solid lines). The lines guide the eye.

vibron; its computed frequencies are in the range 1370–1480  $\text{cm}^{-1}$ , which, while slightly lower than found in experiment [11], *increase* with increasing pressure in qualitative accordance with measurements and a decreasing dimer length. The  $B_{2u}$  mode is an antiphase libronlike mode with frequencies between 465–703  $\text{cm}^{-1}$  over the pressure range 8–86 GPa. As with the vibron, these frequencies are somewhat larger than those found experimentally, which increase from 300 to 600  $\text{cm}^{-1}$  between 10 and 70 GPa at room temperature [10,11], a discrepancy that likely originates from the smaller  $\text{O}_2\text{-O}_2$  distance we calculate. Since the decline in intermolecular distance associated with the  $Cmcm$  phase results in an increasingly covalent intermolecular bond, significant changes in dynamical effective charges (and hence absorptivity) may then be expected on entry into this new phase.

The Raman-active vibron ( $A_g$ ) is in the range 1500–1650  $\text{cm}^{-1}$ , also in good agreement with measurement. Additionally, we predict five other Raman-active intermolecular modes, and two can ostensibly be assigned to observed peaks below 500  $\text{cm}^{-1}$  [11,34], the  $B_{3g}$  and lowest-frequency  $B_{2g}$  modes. Since our calculations overestimate the IR-active mode frequencies, we regard this specific assignment as tentative. Extended scattering geometries with fully polarized radiation may be needed to elucidate three further Raman-active modes predicted here whose intensities may be weak, given the normal mode displacement patterns associated with the linear structure and given the very anisotropic molecular polarizability. In this context we note that the modes of interest are close in frequency to observed Raman peaks [34] which have been assigned, so far, to possible overtones and combinations of librations. It is also worth noting that even more modes would be expected of a more complicated  $\epsilon$  phase, should it have a larger unit cell. Our results therefore suggest that an assessment of the phase diagram and lattice dynamics at low temperatures and over a wide pressure range will be of considerable experimental interest.

We gratefully acknowledge M. H. Cohen, M. P. Teter, and D. Vanderbilt for useful commentary, and we thank G. Kresse for providing the PAW potentials. This work was supported by the National Science Foundation (DMR-9988576). This work made use of the Cornell Center for Materials Research Shared Experimental Facilities, supported through the National Science Foundation Materials Research Science and Engineering Centers program (DMR-9632275).

- 
- [1] R. J. Meier and R. B. Helmholdt, Phys. Rev. B **29**, 1387 (1984).
  - [2] M. Nicol and K. Syassen, Phys. Rev. B **28**, 1201 (1983).
  - [3] D. Schiferl *et al.*, Acta Crystallogr. Sect. B **39**, 153 (1983).
  - [4] Y. Akahama *et al.*, Phys. Rev. Lett. **74**, 4690 (1995).
  - [5] S. Desgreniers, Y. K. Vohra, and A. L. Ruoff, J. Phys. Chem. **94**, 1117 (1990).

- [6] M. Bastea, A. C. Mitchell, and W. J. Nellis, Phys. Rev. Lett. **86**, 3108 (2001).
- [7] K. Shimizu *et al.*, Nature (London) **393**, 767 (1998).
- [8] M. F. Nicol, K. R. Hirsch, and W. B. Holzapfel, Chem. Phys. Lett. **68**, 49 (1979).
- [9] F. A. Gorelli *et al.*, Phys. Rev. Lett. **83**, 4093 (1999).
- [10] Y. Akahama and H. Kawamura, Phys. Rev. B **61**, 8801 (2000).
- [11] F. A. Gorelli *et al.*, Phys. Rev. B **63**, 104110 (2001).
- [12] B. Edwards and N. W. Ashcroft, Nature (London) **388**, 652 (1997).
- [13] S. W. Johnson, M. Nicol, and D. Schiferl, J. Appl. Crystallogr. **26**, 320 (1993).
- [14] S. Desgreniers and K. E. Brister, in *High Pressure Science and Technology*, edited by W. A. Trzeciakowski (World Scientific, Singapore, 1996), p. 363.
- [15] S. F. Agnew, B. I. Swanson, and L. H. Jones, J. Chem. Phys. **86**, 5239 (1987).
- [16] Y. Akahama, H. Kawamura, and O. Shimomura, Phys. Rev. B **64**, 054105 (2001).
- [17] R. Gebauer *et al.*, Phys. Rev. B **61**, 6145 (2000).
- [18] S. Serra *et al.*, Phys. Rev. Lett. **80**, 5160 (1998).
- [19] P. Hohenberg and W. Kohn, Phys. Rev. **136**, 864B (1964); W. Kohn and L. J. Sham, Phys. Rev. **140**, 1133A (1965).
- [20] J. P. Perdew *et al.*, Phys. Rev. B **46**, 6671 (1992); S. H. Vosko, L. Wilk, and M. Nusair, Can. J. Phys. **58**, 1200 (1980).
- [21] P. Blöchl, Phys. Rev. B **50**, 17 953 (1994); G. Kresse and D. Joubert, Phys. Rev. B **59**, 1758 (1999).
- [22] G. Kresse and J. Hafner, Phys. Rev. B **47**, 558 (1993); G. Kresse and J. Furthmüller, Comput. Mater. Sci. **6**, 15 (1996).
- [23] J. P. Perdew, K. Burke, and M. Ernzerhof, Phys. Rev. Lett. **80**, 891 (1998); F. W. Kutzler and G. S. Painter, Phys. Rev. B **45**, 3236 (1992).
- [24] *Landolt-Börnstein: Numerical Data and Functional Relationships in Science and Technology*, Group I, edited by A. Eucken (Springer-Verlag, Berlin, 1951), Vol. 3, p. 510.
- [25] See R. D. Eppers, K. Kobashi, and J. Belak, Phys. Rev. B **32**, 4097 (1985), and references therein.
- [26] K. Rapcewicz and N. W. Ashcroft, Phys. Rev. B **44**, 4032 (1991).
- [27] W. Kohn, Y. Meir, and D. E. Makarov, Phys. Rev. Lett. **80**, 4153 (1998).
- [28] J. Yen and M. Nicol, J. Phys. Chem. **91**, 3336 (1987).
- [29] Relaxation of larger supercells containing up to 36 randomly displaced molecules (constructed from four-molecule orthorhombic cells tripled along [100] and [010]) did not result in phases with lower enthalpy.
- [30] Our predicted lattice parameters for antiferromagnetic  $Fmmm$  below 20 GPa yield  $b/a \sim 0.95$  and  $c/a \sim 2$ . Above 50 GPa, nonmagnetic  $C2mm$  is very nearly molecular close-packed, and  $b/a \sim 0.58$  and  $c/a \sim 1.67$ .
- [31] L. Hedin, Phys. Rev. **139**, A796 (1965); M. S. Hybertsen and S. G. Louie, Phys. Rev. B **34**, 5390 (1986).
- [32] M. Santoro *et al.*, Phys. Rev. B **64**, 064428 (2001).
- [33] SMODES was developed by H. T. Stokes and D. M. Hatch. See <http://128.187.18.10/~stokesh/smodes.html>.
- [34] Y. Akahama and H. Kawamura, Phys. Rev. B **54**, R15602 (1996).